

We are IntechOpen, the world's leading publisher of Open Access books Built by scientists, for scientists

6,900

Open access books available

186,000

International authors and editors

200M

Downloads

Our authors are among the

154

Countries delivered to

TOP 1%

most cited scientists

12.2%

Contributors from top 500 universities



WEB OF SCIENCE™

Selection of our books indexed in the Book Citation Index
in Web of Science™ Core Collection (BKCI)

Interested in publishing with us?
Contact book.department@intechopen.com

Numbers displayed above are based on latest data collected.
For more information visit www.intechopen.com



Overview of Important “Organs at Risk” (OAR) in Modern Radiotherapy for Head and Neck Cancer (HNC)

Trinanjana Basu and Nithin Bhaskar

Additional information is available at the end of the chapter

<http://dx.doi.org/10.5772/intechopen.80606>

Abstract

With the advent of highly conformal and adaptive radiotherapy techniques, the significance of accurate delineation of organs at risk (OARs) is becoming more and more important. Techniques such as Intensity modulated radiotherapy (IMRT) and intensity/volumetric modulated arc therapy (VMAT) has allowed for improved dose conformation within the target. It has also allowed for steep dose gradients around the target for better normal tissue sparing. The accurate contouring and delineation of the OARs are thus warranted as variation in delineation has been systematically reported in studies. All these facts have led to the development of contouring guidelines for OARs in various sites. Head and neck cancers (HNC) are a perfect example where outcome and quality of life (QOL) balance remains a therapeutic challenge. There are several OARs and thus the accurate delineation following a standard guideline becomes more important. This chapter looks into the published guidelines for the delineation of such structures.

Keywords: head and neck cancer, IMRT, VMAT, QOL, organs at risk

1. Introduction

The variation in the contouring and delineation of the different OAR's has been systematically reported in studies [1]. We will be discussing the standard available guidelines and a simple practical way to delineate OAR's in modulated radiotherapy for HNC. The OAR's have been divided into five subgroups viz. optic structures, salivation related structures, structures related to swallowing, brachial plexus and intra-cranial structures.

2. Optic structures

2.1. Eye ball

The entire eye ball is to be contoured as a single structure. The entire retina is to be included.

For contouring of substructures of the eye the European particle therapy network (EPTN) has put forward a consensus based atlas based on CT and MRI [2].

2.1.1. Cornea

The cornea is located anterior to the vitreous humor, iris, lens and ciliary body [2]. It can be delineated in MRI or CT and is contoured with a 2-3 mm brush.

RT can injure the cornea by damaging the deeper layers of stroma, but in most cases the acute toxicity is as a result of loss of tear film [3].

Dose recommendation: < 40 Gy. Edema of the corneal stroma appears at a dose of 40-50Gy, but is usually transient. With doses of 60 Gy the chance of corneal ulceration is increased to 17–20% which increases further if chemotherapy is added.

2.1.2. Retina

It is the innermost layer of the globe and is about 0.25 mm in thickness and is not usually visualized in a standard MRI [2]. Contoured using a 3 mm brush, the retina covers the posterior 5/6th of the globe. The optic nerve is not contoured along with it [4].

Dose recommendations: Dmax—45Gy. Acute retinal toxicity is not reported. Being a part of the central nervous system, the retina behaves as a late reacting tissue [3]. Usually there is a latent period of 6 months to 3 years before the onset of clinically significant retinopathy. The mean latent period is 19 months [5].

2.1.3. Lens

Biconvex structure in the aqueous humor, it is clearly visible in CT [2]. The structure is about 10 mm in diameter seen in the coronal plane.

Dose recommendations: Dmax—5 to 10 Gy. Acute lens toxicity is not reported. A single dose of 2 Gy can cause cataract, but is usually visually insignificant. [3] The time of onset is dose related. For doses in the range of 2.5–6.5Gy, the latency is 8 yrs. with the possibility of 33% progressive cataract, whereas doses of 6.5–11.5Gy, the latency reduces to 4 years with the 66% risk of progressive cataract.

2.2. Optic nerve

While moving craniocaudally, optic nerve is seen below the superior rectus. The nerve is 2-5 mm thick and is delineated from the posterior margin of retina and continued along its course posteriorly till it merges with the optic chiasm after passing through the superior orbital fissure.

Dose recommendations: Dmax <54 Gy. The incidence of radiation induced optic neuropathy (RION) is unusual for doses less than 55 Gy. At 55–60 Gy the risk becomes 3–7% and for doses >60 Gy the risk is quite significant at 7–20% [6].

2.3. Optic chiasm

A small structure is usually confined to 2 or 3 slices in the superior-inferior direction. Better demarcated in MRI, the chiasm is situated about 1 cm superior to the pituitary gland. Laterally it is bounded by the carotid arteries. It is better visible in MRI with a high signal on T1. A good landmark to look for is the pituitary stalk. It lies just posterior to the chiasm and appears hyperintense even on plain CT [7]. On average it measures 8 x 14 mm (APxTrans) and is about 2–5 mm thickness in the super-inferior dimension [7].

It should be kept in mind that, the chiasm should be contoured in continuity with the optic nerves.

Dose recommendations: D max <54 Gy [6].

2.4. Lacrimal gland

Freedman et al. [8] has given a step-by-step instruction to contour the lacrimal gland. The contour starts by identifying the mid portion of the gland and thereafter tracking it superiorly and inferiorly.

Superior extend corresponds to the super-lateral corner of orbit, just below the orbital rim. Inferiorly it does not extend below the level of insertion of lateral rectus.

The gland is better delineated in brain (120/40) or soft tissue (350/50) window.

Dose recommendations: Dmean <30 Gy. Doses above 40 Gy have shown to steeply increase the incidence of dry eye while doses above 57–60Gy can cause permanent loss of tearing [9].

The details are given in **Figures 1–3**.

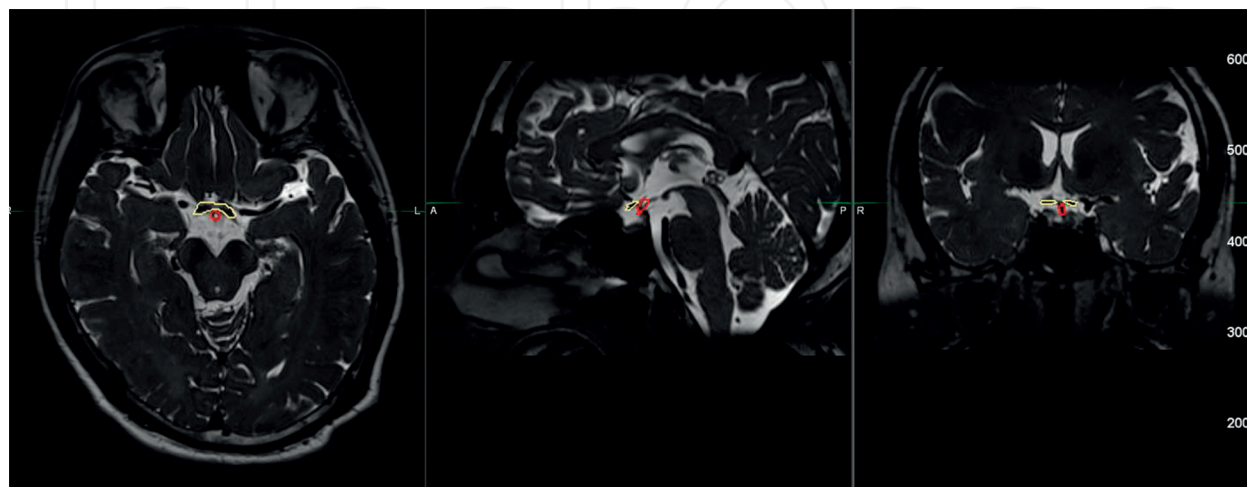


Figure 1. Optic apparatus.

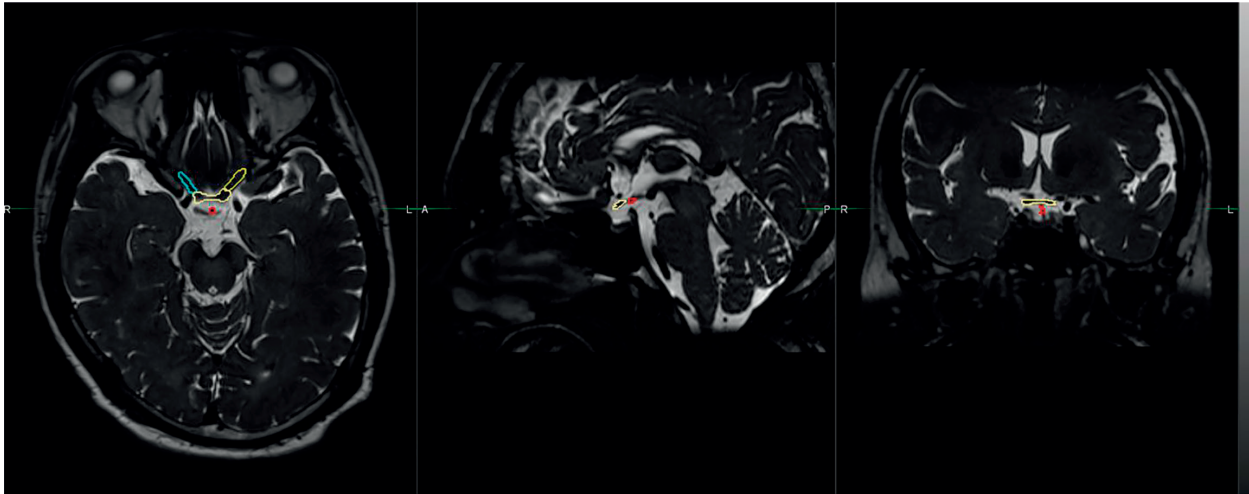


Figure 2. Optic chiasm.

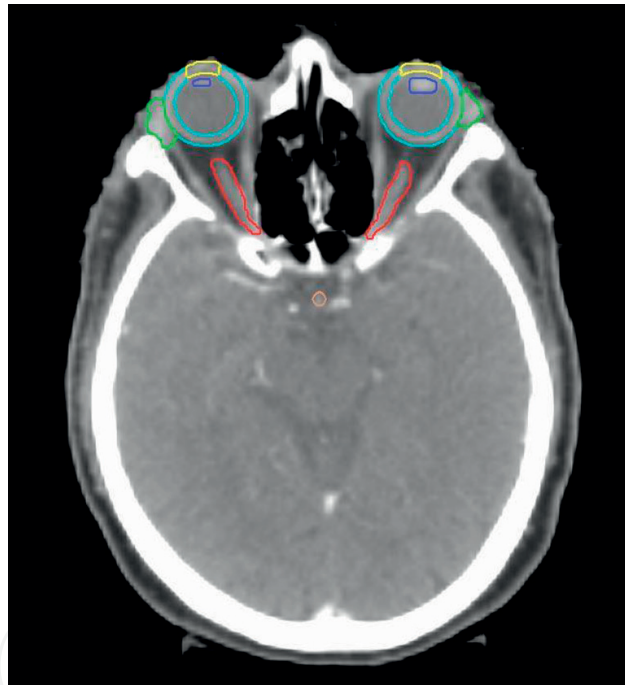


Figure 3. Eye balls and associated structures.

3. Salivation related structures

3.1. Parotids

Parotids are contoured based on the guidelines given by Water et al. [10] (**Table 1**). It is to be noted that in 20% of the cases, the parotid gland extends anteriorly over the surface of the masseter muscle following the parotid duct and in the anterior direction the deep lobe of the parotid gland may extend alongside the medial border of the mandible gland may extend

OAR	Anatomic boundaries					
	Cranial	Caudal	Anterior	Posterior	Lateral	Medial
Parotid gland	External auditory canal, mastoid process	Posterior part of submandibular space	Masseter muscle, posterior mandible, medial and lateral pterygoid muscle	Anterior belly of SCM muscle,	Subcutaneous place, platysma muscle	Posterior belly of digastric muscle, styloid, parapharyngeal space
Submandibular gland	Medial pterygoid muscle, mylohyoid muscle	Subcutaneous fat	Mylohyoid muscle, lateral surface, hyoglossus muscle	Parapharyngeal space, SCM	Mandible (medial border), platysma, medial surface of medial pterygoid	Superior and middle PCM, anterior belly of digastric muscle, mylohyoid muscle (lateral surface), hyoglossus muscle
Sublingual gland	Mucus membrane covering FOM	mylohyoid muscle, geniohyoid muscle	Mandible, mylohyoid muscle	Hyoglossus muscle	Medial surface of mandibular bone, mylohyoid muscle	Genioglossus muscle
Soft palate	Hard palate, nasopharynx (air space)	BOT, Tonsils, oropharynx (air space)	HP, BOT/tongue, oral cavity (airspace)	Pharynx (mucosal surface/airspace), superior PCM	Pterygoid process, medial pterygoid plate, superior PCM, medial pterygoid m., PPS, palatine tonsil, pharyngeal lumen	
Upper lip glands	Hard palate, nasal spine	lower end of upper lip	Orbicularis oris muscle, subcutaneous tissue/fat	Teeth, maxillary bone, HP, tongue	Depressor anguli oris muscle, buccinator muscle, levator anguli oris muscle/risorius muscle	
Lower lip glands	Upper edge of lower lip	lower edge of teeth sockets/mandibular body	Orbicularis oris muscle, subcutaneous tissue/fat	Teeth, mandible, tongue/air	Depressor anguli oris muscle, buccinator muscle,	
Buccal mucosa glands	Line between maxillary process and alveolar process of maxilla	Alveolar process of mandible	Orbicularis oris muscle	Posterior edge of mandibular body and maxilla	Buccinator muscle, subcutaneous fat	Mandible, teeth, tongue

SCM—sternocleidomastoid, PCM—pharyngeal constrictor muscle, BOT—base of tongue, HP—hard palate, FOM—floor of mouth.

Table 1. Salivation related structures.

alongside the medial border of the mandible. The external carotid artery, the retromandibular vein and the extracranial facial nerve are enclosed in the parotid gland.

The external carotid artery (ECA), retromandibular vein and the extra-cranial part of facial nerve are enclosed in the gland. If contrast agents are used, the vessels can be clearly demarcated and can be avoided from the gland contour. But as contrast administration is not routinely practiced, and to make the contouring practice uniform, it is recommended to include the vessels within the gland contour.

Dose recommendations: severe xerostomia or salivary output <25% of baseline can be avoided if at least one parotid is restricted to a mean dose <20 Gy or both parotids restricted to <25 Gy [11].

3.2. Submandibular gland

Situated in the floor of the mouth, it is a predominantly serous gland having a large superficial lobe and a small deep process separated by the fibers of mylohyoid. In most cases the gland is hypo dense on CT and can be easily demarcated.

Dose recommendations: if deemed oncologically safe, the mean dose to the submandibular gland, restricted to 35Gy may reduce xerostomia symptoms [11].

3.3. Sublingual gland

Sublingual gland is the smallest of the three major salivary glands. It is a predominantly mucus gland, situated in the anterior part of oral cavity in the sublingual space.

3.4. Extended oral cavity

The extended oral cavity is contoured partly based on the work by Hoebbers et al. [12] excluding the lips and buccal mucosa [4]. It includes the space posterior to the arch of mandible and maxilla. Posteriorly it is limited by the uvula, soft palate and the base of tongue.

3.4.1. Soft palate

Soft palate contains numerous minor salivary glands. It is better seen in the sagittal sections by a thin air line separating it from the tongue inferiorly. As the salivary glands are distributed along the length of the soft palate, the entire soft palate is contoured including the uvula.

Dose recommendations: oral cavity dose should be kept as low as possible. Seeking for V45 < 40% and V50 < 20% limits mucositis and improves QoL [12].

3.5. Other minor salivary glands

These glands are distributed along the inner aspects of lips and buccal mucosa between the mucous membrane and the muscle layer. Maximum depth from the mucosal surface is about 4 mm with lower lip glands deeper than the upper ones.

3.5.1. Lower lip glands

The upper and posterior limit of the lip is better identified in sagittal sections. The lower limit corresponds to the caudal limit of teeth sockets or the cranial mandibular body (in case of edentulate mandible) [10].

3.5.2. Upper lip glands

As of the lower lip, the lower and posterior extend is more easily made out in the sagittal plane. Cranially it extends till the nasal spine [10].

Dose recommendations: seek for a lip dose less than the oral cavity dose. A mean dose of 30Gy and 50 Gy for oral cavity and non-oral cavity cancers respectively would be preferable.

Orbicularis oris muscle can be used to delineate the glands anteriorly.

3.5.3. Glands of buccal mucosa

The glands of buccal mucosa are difficult to distinguish. The cranial, caudal and medial borders are better visualized in the coronal plane.

The abovementioned have been summarized in **Table 1**: salivation-related structures.

4. Swallowing related structures

4.1. Pharyngeal constrictor muscles

Pharyngeal wall has two layers of muscle (**Table 2**). The outer circular layer which are the pharyngeal constrictor muscles (PCM) and inner longitudinal muscles which are levators (stylopharyngeus and palatopharyngeus). PCM has three parts—superior, middle and inferior constrictor. The caudal ends of the levators blend with the PCM. These muscles are usually hard to differentiate from PCM and are not contoured differently.

4.1.1. Superior PCM

They originate from sphenoid bone from its pterygoid hamulus and insert to the median raphe. Different authors have put forward different levels in regards to its cranial border. Generally, cranial border of the superior PCM is taken as the caudal tip of the pterygoid plate, i.e., the pterygoid hamulus. The lowest fibers of the superior PCM are separated by the middle PCM by stylopharyngeus and glossopharyngeal nerve. These fibers also overlap onto the upper fibers of middle PCM. As these changes are hardly made out in CT, most authors define the lowest limit of the muscle as the cranial border of hyoid bone. But this can lead to missing of half of middle PCM. Thus, the cranial border can be considered at the lower border of second cervical vertebra.

Organ at risk	Anatomic boundaries					
	Cranial	Caudal	Anterior	Posterior	Lateral	Medial
Superior PCM	Inferior tip of pterygoid hamulus	Inferior edge of C2	Pterygoid hamulus, BOT, pharyngeal lumen	Prevertebral muscles	Medial pterygoid muscles	Pharyngeal lumen
Middle PCM	Superior edge of C3	Inferior edge of hyoid	BOT, hyoid	Prevertebral muscles	Hyoid—greater horn. Thyroid cartilage—superior horn	Pharyngeal lumen
Inferior PCM	First slice inferior to inferior edge of hyoid	Inferior edge of arytenoid cartilage	Soft tissue of supraglottis/glottis	Prevertebral muscles	Superior horn of thyroid cartilage	
Cricopharyngeal muscle	First slice inferior to arytenoid cartilage	Inferior edge of cricoid	Posterior edge of cricoid	Prevertebral muscles	Thyroid gland/cartilage, fatty tissue	
EIM	First slice inferior to cricoid	1 cm inferior to the upper extend	Tracheal lumen	Prevertebral muscles	Thyroid gland, fatty tissue	
Cervical esophagus	1 cm inferior to the cricoid	Sternal notch				
BOT	Inferior edge of C1	Superior edge of hyoid	Posterior 1/3 from mandibular bone to pharyngeal lumen	Pharyngeal lumen	Width of the lumen of pharynx	
Supraglottic larynx	Tip of epiglottis	First slice superior to the arytenoid cartilage	Hyoid, thyroid cartilage, preepiglottic space	Pharyngeal lumen, inferior PCM	Thyroid cartilage	Pharyngeal lumen (lumen to be excluded)
Glottic larynx	Superior edge of arytenoid cartilage	Inferior edge of cricoid cartilage (only the soft tissue element)	Thyroid cartilage	Inferior PCM, pharyngeal lumen/cricoid	Thyroid cartilage	Pharyngeal lumen (lumen to be excluded)

Table 2. Swallowing related structures.

4.1.2. Middle PCM

The fibers originate from the greater and lesser horns of hyoid bone and insert along the median raphe. The upper fibers overlap, therefore these boundaries are arbitrary. The upper border is taken as the lower border of superior PCM. Lower border corresponds to the lower border of hyoid bone.

4.1.3. Inferior PCM

The thickest of the three constrictors, the inferior PCM has two parts—the thyropharyngeal part which originate from the oblique line of thyroid cartilage and the cricopharyngeal part which originate from the lateral part of thyroid cartilage. Most authors delineate these two structures separately. The thyropharyngeus is referred to as inferior PCM and the latter is referred to as cricopharyngeal muscle. As functionally these muscles are different, they are contoured differently.

The inferior PCM starts cranially from the caudal end of middle PCM, usually one slice below the caudal end of hyoid. The caudal border corresponds to the upper border of cricoid, just below the level of arytenoid.

Anteriorly, the inferior PCM attaches to the posterior edge of thyroid cartilage, which can be recognized easily on CT, while the posterior border is defined by the prevertebral muscles.

Dose recommendations: $D_{\text{mean}} < 50 \text{ Gy}$.

4.1.4. Cricopharyngeus

Delineation starts cranially one slice below the level of arytenoids which also corresponds to the lower limit of inferior PCM. The contour continues till the lower end of cricoid cartilage.

4.2. Esophageal inlet muscles (EIM)

Levendag et al. [10] recommends contouring the proximal 1 cm of esophagus as a separate structure. The cranial border starts from the caudal end of cricopharyngeus.

4.3. Cervical esophagus (CE)

The contouring of CE varies from authors [13, 14]. For the purpose of consistency the upper border of CE starts 1 cm below the esophageal inlet muscles and end at the level of sternal notch.

4.4. Base of tongue (BOT)

The delineation of BOT has been provided by three authors. All of them are consistent with the cranial extend defined as just below the soft palate. As this boundary is difficult to identify in CT, the lower end of anterior tubercle of C1 vertebra (which corresponds to the same level) may be taken for the demarcation. The three authors vary in the definition of the lower

extend. The lower limit of hyoid [13], the vallecular and the first slice of epiglottis [14] are mentioned, but for consistency, we follow the upper end of body of hyoid as the lower caudal limit of BOT.

4.5. Contouring of larynx structures

Freedman et al. [15] has provided a 3 step method to delineate larynx. Step 1 and 3 identifies the cranial and caudal limit of larynx. The contouring starts from the slice just below the caudal edge of hyoid and ends where the cricoid cartilage is seen as a complete ring. Step 2 mentions the circumference limits of the larynx. The anterior border corresponds to the inner surface of the thyroid cartilage. The posterior border in the upper part corresponds to the lateral surfaces of the aryepiglottic folds and the posterior surface of the mucosa covering the arytenoids. In the lower part it corresponds to the posterior surface of the cricoid cartilage. The pyriform sinus is not to be included in the contour.

The above guidelines contour the larynx as a single structure. As the larynx consists of subglottic, glottic and the supraglottic area, several authors have delineated these sub-sites separately. The supraglottis includes the epiglottis, the aryepiglottic folds, the arytenoids, and the false vocal cords. The glottis is composed of the true vocal cords and the subglottis extends from lower end of glottis to lower edge of cricoid.

The delineation of supraglottis and glottis is based on the function of the two subsites. While the supraglottis includes the muscles responsible for the closure of larynx, the glottis part is responsible for the movement of the vocal cords.

4.5.1. Supraglottic larynx

The contour includes the supraglottic adductors (oblique arytenoids and aryepiglottic muscles) and epiglottis. The cranial border is the tip of the epiglottis and the contour continues inferiorly till the upper edge of arytenoid cartilage.

4.5.2. Glottis

The contour starts from the upper end of arytenoid cartilage and ends caudally at the lower edge of the cricoid. Only the soft tissue is contoured (except for the arytenoids). The cricoid and the thyroid cartilage should be excluded.

Dose recommendations: To minimize laryngeal edema, the volume of larynx receiving 50 Gy and mean dose should be kept as low as possible, ideally $\leq 20\%$ and 40 Gy respectively [16].

The above has been summarized in **Table 2:** Swallowing related structures.

5. Brachial plexus

Guidelines for contouring brachial plexus has been put forward by Hall et al. They have put forward step-by-step technique. The contour starts from the neural foramina of C5-T1.

It extends from outer edge of spinal canal to the space between anterior and middle scalene. Where no spinal foramina was present, only the space between anterior and middle scalene is contoured. The middle scalene will end in the region of the subclavian neurovascular bundle. In the lower part, the brachial plexus is contoured in the posterior aspect of neurovascular bundle in the inferior and lateral aspect one to two slices below the clavicle.

Dose recommendations: Dmax <60Gy. Emami et al. [17] has suggested TD 5/5 for the entire brachial plexus to be 60Gy. More recent studies with longer follow-up (upto 20 years) have shown that the risk of plexopathy keeps rising even after 5 yrs. and may not be apparent until 20 years after radiation [18].

6. Intra cranial structures

6.1. Ear structures

Ear structures (both the middle ear and inner ear) should be contoured using the bone window.

6.1.1. Middle ear

The eustachian tube (ET), tympanic cavity and the mastoid air cells (M) may be contoured separately based on the CT/MRI anatomy.

Dose recommendations: ET $D_{30} < 52\text{Gy}$; M $D_{0.05\text{cc}} < 41\text{ Gy}$. Based on the study by Yao et al. [19], dose to 30% of ET and 0.5 cc of mastoid volume were the main predictors of severe ear disorders. Doses above these are associated with increase in grade 2 ear disorders post RT.

6.1.2. Cochlea

It is a small spiral structure of about 0.6cm^3 volume located in the petrous part of temporal bone. The small bony cavity can be visualized better with a setting of 120/1500 on CT. The structures of inner ear are visualized more in T2 weighted MRI images. The semicircular canals should not be contoured.

Dose recommendations: Dmean <45 Gy. In children it is advisable to keep it below 35 Gy. [20]

6.1.3. Vestibular and semicircular canal

Arranged in 3 planes, the canals are contoured in bone window (120/1500). They are located lateral and superior to the cochlea.

6.2. Brain stem

Brain stem comprises of midbrain, pons and medulla. The cranial extend starts from the level of inferior section of lateral ventricle. The organ is better visualized better in MRI. The contour extends till the level of the tip of dense of C2 vertebra or foramen magnum.

6.2.1. Midbrain

It starts from the nigral substance of the cerebral peduncle and ends upper border of pons.

6.2.2. Pons

Better visualized as an oval structure in sagittal sections, it is easily delineated.

6.2.3. Medulla

Medulla starts from the lower end of pons to the level of tip of dense of axis.

Dose recommendations: Dmax—54 Gy. The entire brain stem can be treated to a dose of 54 Gy with little risk of serious side effects. [21]. Mean time of onset of symptom is 17 months (range 4.5–19 months). Smaller volumes (1-10 cc) may be irradiated to 59Gy at fractionations ≤ 2 Gy [22].

6.3. Pituitary gland

A small gland, it is difficult to visualize in CT, but sella turcica can be used as a surrogate marked and the inner boundary of the same can be contoured for its delineation. The gland lies immediately below the brain and is connected to the hypothalamus by its stalk.

CT density of pituitary gland is similar to brain. Upon contrast administration, the gland may become more hyperintense than brain due to the rich vascular supply.

Dose recommendations: DMax 45Gy (for pan hypopituitarism, lower for Growth hormone (GH) deficiency). The anterior pituitary has 5 different types of cells, each with different radiosensitivity. Most sensitive is the GH axis followed by the gonadotropin, ACTH and TSH axis. GH deficiency has been noted in relatively lower doses, and has been reported for TBI for doses as low as 10 Gy [23], but the incidence increases substantially after 30 Gy where the incidence can be as high as 50–100%.

6.4. Temporal lobe

Contouring of temporal lobe should include the hippocampus, parahippocampal gyrus and the uncus. The basal ganglia and insula are excluded from the contour. Cranially it starts for the superior end of sylvian fissure and ends inferiorly at the base of middle cranial fossa. Medial boundary is marked by cavernous sinus, sphenoid sinus and the sylvian fissure and laterally by the temporal bone.

7. Discussion

The modern radiotherapy in HNC have revolutionized treatment outcome especially in terms of acute and late toxicity. It thus brings about a clear change in treatment outcome. One important aspect in preserving the QOL is the OAR's. We, as radiation oncologist are much

aware about the importance of accurate delineation of these structures. Only an accurate delineation can lead to effective sparing and thus a desirable outcome in terms of QOL. There were several isolated guidelines available. In this chapter we tried to summarize all the available guidelines. For certain organs like temporal lobe, multiple guidelines are available in the literature. We have tried to incorporate them together to put forward a single uniform consensus. Having said that the delineation and the attempted dose constraints should also be evaluated based on the target volume and tumor control. In case of parallel structures, the target volume coverage should be made priority and the risks and side effects of the same should be communicated to the patients. In such cases the volume of OARs outside the planning target volume (PTV) may be delineated separately and similar dose constraints may be aimed for. It should also be kept in mind that even with the most sophisticated of technologies, not all of the dose constraints might not be achieved due to the basic physics of the photon beam. In such situations a trade-off should be agreed upon. However, such liberties, should not be attempted with serial structures like spinal cord and brain stem. Organs such as these should always be given hard constraints. If the PTV is overlapping such structures, under dose the area is accepted.

8. Conclusion

The chapter summarizes basic day to day information for a radiation oncologist to delineate OAR's in HNC radiotherapy. There are several updates and the readers are encouraged to go through them at a regular interval. We will be publishing a detail clinical end point based acute and late toxicities of these OAR's at a later date.

Acknowledgements

The second opportunity to work with IntechOpen publishers has been excellent. I must thank my colleague Dr. Nithin in crafting the manuscript and it was his enthusiasm which led to a detail manuscript. We both would like to thank our respective parents for all the support and blessings. My wife (Reshmi) and Nithin's wife (Dr. Nikhila) respectively have been the greatest source of support. We also would like to thank our organization (HCG Apex Cancer Centre in Mumbai, India) for encouraging academic engagements in all possible aspects.

Author details

Trinanjana Basu* and Nithin Bhaskar

*Address all correspondence to: trinanjana.doctor@gmail.com

Department of Radiation Oncology, HCG Apex Cancer Centre, Mumbai, India

References

- [1] Brouwer CL, Steenbakkers RJHM, van den Heuvel E, Duppen JC, Navran A, Bijl HP, et al. 3D variation in delineation of head and neck organs at risk. *Radiation Oncology* [Internet]. 2012 Mar 13 [cited 2018 Apr 23];7:32 Available from: <http://www.ncbi.nlm.nih.gov/pubmed/22414264>
- [2] Eekers DB, In't Ven L, Roelofs E, Postma A, Alapetite C, Burnet NG, et al. The EPTN consensus-based atlas for CT- and MR-based contouring in neuro-oncology. *Radiotherapy Oncology* [Internet]. 2018 Mar 13 [Cited 2018 May 5];0(0) Available from: <http://www.ncbi.nlm.nih.gov/pubmed/29548560>
- [3] VSE J, Wirth A, Mac Manus MP. Ocular risks from orbital and Periorbital radiation therapy: A critical review. *International Journal of Radiation Oncology* [Internet]. 2011 Mar [cited 2018 Jul 14];79(3):650-659 Available from: <http://linkinghub.elsevier.com/retrieve/pii/S0360301610034619>
- [4] Brouwer CL, Steenbakkers RJHM, Bourhis J, Budach W, Grau C, Grégoire V, et al. CT-based delineation of organs at risk in the head and neck region: DAHANCA, EORTC, GORTEC, HKNPCSG, NCIC CTG, NCRI, NRG oncology and TROG consensus guidelines. *Radiotherapy Oncology* [Internet]. 2015 Oct [cited 2018 Jul 12];117(1):83-90 Available from: <http://www.ncbi.nlm.nih.gov/pubmed/26277855>
- [5] Brown GC, Shields JA, Sanborn G, Augsburger JJ, Savino PJ, Schatz NJ. Radiation retinopathy. *Ophthalmology* [Internet]. 1982 Dec [cited 2018 Jul 14];89(12):1494-1501 Available from: <http://linkinghub.elsevier.com/retrieve/pii/S0161642082346114>
- [6] Mayo C, Martel MK, Marks LB, Flickinger J, Nam J, Kirkpatrick J. Radiation dose-volume effects of optic nerves and chiasm. *International Journal of Radiation Oncology Biology Physics* [Internet]. 2010 Mar 1 [cited 2018 Jul 12];76(3 Suppl):S28-S35 Available from: <http://www.ncbi.nlm.nih.gov/pubmed/20171514>
- [7] Scoccianti S, Detti B, Gadda D, Greto D, Furfaro I, Meacci F, et al. Organs at risk in the brain and their dose-constraints in adults and in children: A radiation oncologist's guide for delineation in everyday practice. *Radiotherapy Oncology* [Internet]. 2015 Feb 1 [cited 2018 Jul 12];114(2):230-238 Available from: <https://www.sciencedirect.com/science/article/pii/S0167814015000808>
- [8] Freedman L, Sidani C. A radiation Oncologist's guide to contouring the lacrimal gland. *Practical Radiation Oncology* [Internet]. 2015 Nov 1 [cited 2018 May 4];5(6):e697-e698 Available from: <http://linkinghub.elsevier.com/retrieve/pii/S1879850015002076>
- [9] Parsons JT, Bova FJ, Mendenhall WM, Million RR, Fitzgerald CR. Response of the normal eye to high dose radiotherapy. *Oncology (Williston Park)* [Internet]. 1996 Jun [cited 2018 Jul 14];10(6):837-47-8, 851-2 Available from: <http://www.ncbi.nlm.nih.gov/pubmed/8823799>

- [10] van de Water TA, Bijl HP, Westerlaan HE, Langendijk JA. Delineation guidelines for organs at risk involved in radiation-induced salivary dysfunction and xerostomia. *Radiotherapy Oncology* [Internet]. Available from. 2009;**93**(3):545-552. DOI: 10.1016/j.radonc.2009.09.008
- [11] Deasy JO, Moiseenko V, Marks L, Chao KSC, Nam J, Eisbruch A. Radiotherapy dose-volume effects on salivary gland function. *International Journal of Radiation Oncology Biology Physics* [Internet]. 2010 Mar 1 [cited 2018 Jul 14];**76**(3 Suppl):S58-S63 Available from: <http://www.ncbi.nlm.nih.gov/pubmed/20171519>
- [12] Hoebbers F, Yu E, Eisbruch A, Thorstad W, O'Sullivan B, Dawson LA, et al. A pragmatic contouring guideline for salivary gland structures in head and neck radiation oncology. *American Journal of Clinical Oncology* [Internet]. 2013 Feb [cited 2018 Jul 16];**36**(1):70-76 Available from: <http://content.wkhealth.com/linkback/openurl?sid=WKPTLP:landingpage&an=00000421-201302000-00013>
- [13] Dirix P, Abbeel S, Vanstraelen B, Hermans R, Nuyts S. Dysphagia after Chemoradiotherapy for head-and-neck squamous cell carcinoma: Dose-effect relationships for the swallowing structures. *International Journal of Radiation Oncology* [Internet]. 2009 Oct 1 [cited 2018 May 3];**75**(2):385-392 Available from: <http://www.ncbi.nlm.nih.gov/pubmed/19553033>
- [14] Jensen K, Lambertsen K, Grau C. Late swallowing dysfunction and dysphagia after radiotherapy for pharynx cancer: Frequency, intensity and correlation with dose and volume parameters. *Radiotherapy Oncology* [Internet]. 2007 Oct [cited 2018 May 3];**85**(1):74-82 Available from: <http://www.ncbi.nlm.nih.gov/pubmed/17673322>
- [15] Freedman L. A radiation oncologist's guide to contouring the larynx. *Practical Radiation Oncology* [Internet]. 2016 Mar 1 [cited 2018 Apr 30];**6**(2):129-130 Available from: <http://linkinghub.elsevier.com/retrieve/pii/S1879850015003756>
- [16] Rancati T, Schwarz M, Allen AM, Feng F, Popovtzer A, Mittal B, et al. Radiation dose-volume effects in the larynx and pharynx. *International Journal of Radiation Oncology Biology Physics* [Internet]. 2010 Mar 1 [cited 2018 Jul 14];**76**(3 Suppl):S64-S69 Available from: <http://www.ncbi.nlm.nih.gov/pubmed/20171520>
- [17] Emami B, Lyman J, Brown A, Coia L, Goitein M, Munzenrider JE, et al. Tolerance of normal tissue to therapeutic irradiation. *International Journal of Radiation Oncology Biology Physics* [Internet]. 1991 May 15 [cited 2018 Jul 14];**21**(1):109-122 Available from: <http://www.ncbi.nlm.nih.gov/pubmed/2032882>
- [18] Bajrovic A, Rades D, Fehlaue F, Tribius S, Hoeller U, Rudat V, et al. Is there a life-long risk of brachial plexopathy after radiotherapy of supraclavicular lymph nodes in breast cancer patients? *Radiotherapy Oncology* [Internet]. 2004 Jun [cited 2018 Jul 14];**71**(3):297-301 Available from: <http://www.ncbi.nlm.nih.gov/pubmed/15172145>
- [19] Yao J-J, Zhou G-Q, Lin L, Zhang W-J, Peng Y-L, Chen L, et al. Dose-volume factors associated with ear disorders following intensity modulated radiotherapy in nasopharyngeal

carcinoma. *Scientific Reports* [Internet]. 2015 Oct 1 [cited 2018 Jul 16];5(1):13525 Available from: <http://www.nature.com/articles/srep13525>

- [20] Bhandare N, Jackson A, Eisbruch A, Pan CC, Flickinger JC, Antonelli P, et al. Radiation therapy and hearing loss. *International Journal of Radiation Oncology* [Internet]. 2010 Mar 1 [cited 2018 Jul 13];76(3):S50-S57 Available from: <https://www.sciencedirect.com/science/article/pii/S0360301609032982>
- [21] Debus J, Hug EB, Liebsch NJ, O'Farrel D, Finkelstein D, Efird J, et al. Brainstem tolerance to conformal radiotherapy of skull base tumors. *International Journal of Radiation Oncology Biology Physics* [Internet]. 1997 Dec 1 [cited 2018 Jul 14];39(5):967-975 Available from: <http://www.ncbi.nlm.nih.gov/pubmed/9392533>
- [22] Mayo C, Yorke E, Merchant TE. Radiation associated brainstem injury. *International Journal of Radiation Oncology Biology Physics* [Internet]. 2010 Mar 1 [cited 2018 Jul 14];76(3 Suppl):S36-S41 Available from: <http://www.ncbi.nlm.nih.gov/pubmed/20171516>
- [23] Constine LS, Woolf PD, Cann D, Mick G, McCormick K, Raubertas RF, et al. Hypothalamic-pituitary dysfunction after radiation for brain tumors. *The New England Journal of Medicine* [Internet]. 1993 Jan 14 [cited 2018 Jul 14];328(2):87-94 Available from: <http://www.nejm.org/doi/abs/10.1056/NEJM199301143280203>

IntechOpen